A Micromachined Polysilicon Hot-Wire Anemometer

Fukang Jiang, Yu-Chong Tai
Chih-Ming Ho, Wen J. Li**

EE 116-81, Caltech, CA 91125, USA
*MANE, UCLA, Los Angeles, CA 90024, USA

ABSTRACT

Micromachined polysilicon hot-wire anemometers have been designed, fabricated and tested. In comparison to conventional hot-wire anemometers, the new designs feature a wire which is greatly reduced in size. The geometrical structure and material properties of the polysilicon wire have been investigated and optimized to improve the performance of the anemometers. Two types of polysilicon wires with different boron doping profiles were fabricated: centerly lightly doped and uniformly doped. The first type has faster response (2 μs in constant current mode) and higher sensitivity, but the second type shows better stability. In extensive wind tunnel testing, both types have demonstrated faster frequency response, higher spatial resolution and greater sensitivity over conventional counterparts.

1. INTRODUCTION

A hot-wire anemometer is a thermal transducer which is capable of sensing point flow velocity through temperature variation using a heated resistive wire which has a non-zero temperature coefficient of resistance (TCR). When the electrically heated wire is placed in the flow of fluid, the heat is taken away by the flow-induced forced convection. Depending on the operation modes (constant current or constant temperature), either the resistance or the output voltage drop across the wire is a function of the flow velocity.

Conventional hot-wire anemometers have been used for flow velocity measurements for over 80 years. Fig 1(a) shows the structure of a typical hot-wire anemometer. A metal wire is welded or soldered to two metal needles which are molded to the probe body. The wire is usually made of platinum or tungsten and is typically 5 μm in diameter and 1mm in length. It has a resistance of 10 - 30 ohms at room temperature and needs 10 - 40 mA of current to operate[1-2]. These conventional anemometers have to be hand-assembled one by one, thus making it difficult to be arrayed for simultaneous velocity distribution measurement. Also, since the wire diameter is difficult to control with good repeatability, the anemometer probes are essentially not interchangible without recalibrating the whole anemometer system.

Since the spatial resolution of the anemometers for flow velocity distribution measurement is determined by its dimensions, it is advantageous if the wire size can be further reduced. This would also decrease power comsumption and thermal interference to the flow and increase frequency response. In fact, many anemometer designs have been demonstrated using either surface or bulk micromachining technologies[3-7]. Interestingly, however, they are either bulk-micromachined chip-sized devices or wires on top of chips. No one really simulates the real feature of a conventional hot-wire anemometer, i.e., a wire thermistor free-standing in space without anything nearby so that best thermal isolation is achieved. As a result, they can not be direct replacements for the conventional hot-wire anemometers. Here, we report our research on a new type of micromachined anemometers that emphasize the real simulation of a hot-wire anemometer but with greatly reduced wire size. This is made possible by combining surface and bulk micromachining technologies. Not only the spatial resolution and device sensitivity are better, the frequency response is also improved by at least one order of magnitude (confirmed from extensive wind tunnel calibration) over the conventional hot-wire anemometers. Optimization of the structural geometry and the material properties has resulted in anemometers with time constant of 2 μs in the constant current mode (the current record of the time constant for thermal anemometers).

2. DESIGN

Our micromachined hot-wire anemometers have a structure similar to that of conventional hot-wire anemometers. It consists of a sensing wire, two parallel supports, a Si beam, and the thick Si handle, as shown in Fig. 1(b). The Si beam acts as a thermal and mechanical buffer between the supports (0.5 μm thick) and the handle (500 μm thick) to avoid interference with the flow. The sensing wires are about 0.5 μm thick, 1 μm wide, 10-160 μm long, and are free standing to optimize the interaction with the flow and to minimize the thermal conduction to the handle. Polysilicon, instead of platinum or tungsten, is used as the sensing and supporting material because of its compatibility with existing micromachining technologies and because of its controllable TCR in the range of -1%/°C to +0.2%/°C, depending on the doping concentration. The doping concentration of $10^{18}cm^{-3}$ corresponds to a reproducible TCR of -1%/°C for our polysilicon, with which high thermal sensitivity can be achieved even at low operating temperature (shown later).

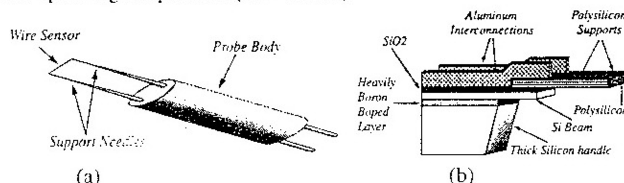

Fig 1. Structures of hot-wire anemometers: (a) Conventional. (b) Micromachined.

The polysilicon wires can be uniformly doped by high dose boron implantation (type I) or nonuniformly doped by a low dose implantation followed by a high dose implantation with the center part of about 2 μm being masked (type II). Type I poly wires behavior similar to the platinum or tungsten wires. For type II wires, the resistance and the ohmic heating are concentrated at the 2 μm lightly doped center region. The other part of the wire acts only as the electrical conductor and mechanical support[8]. It can be expected that anemometers with this type of wire should have improved frequency response and spatial resolution over the type I wires. However, the sensitivity of type II device is not necessarily higher than that of type I device even with a much larger TCR because the temperature change caused by the forced convection may not be as high as that of longer wires. Since the lightly doped part is very short, the total resistance of the anemometer is still within a reasonable range (<20kilo-ohms) which can be adequately handled by signal processing circuits.

3. FABRICATION

It has been reported that polysilicon, deposited in amorphous state and then crystallized has better controllable qualities than as-deposited polysilicon with the deposition temperature at 620°C[9]. We chose to use the former polysilicon, of which the electrical properties were previously calibrated, in the fabrication of our anemometers. We found that its TCR is about 50% higher and the temperature behavior is more linear than the normal poly in the high doping range. Fig 2 shows the resistance changes with temperature for three different types of polysilicon. Moreover, the stress distribution in this polysilicon along the depth is much more uniform, as we will see from the SEM pictures in the late part of this paper. The calibration results show that $2 \times 10^{20}cm^{-3}$ is the doping concentration which gives the lowest sheet resistivity (30Ω/□) and highest positive TCR, and therefore, is the optimum doping concentration for the heavily doped leads in type II anemometers and for the whole wire of the type I anemometers. The doping of the center part (10^{18} cm^{-3}) for type II wire is determined such that the resistance ratio between the center part and the leads is 10 ~ 20 near the operating point. This doping concentration also gives a satisfactory TCR of approximately -1%/ °C. Another factor which needs to be considered for type II is how to avoid lateral diffusion of the boron dopants from the heavily doped leads to the center part during the annealing process which follows after the boron ion implantations. The annealing temperature must not be so high that it causes significant lateral diffusion in the standard 30 min. annealing, but it can not be so low that stable polysilicon resistors could not be made. Therefore, calibration of the lateral boron diffusivity in nonuniformly doped polysilicon was conducted in order to determine the annealing temperature. Fig 3 shows the diffusivity vs. temperature curve. The highest annealing temperature for type II wire is determined to be 900°C from the diffusion model using these data.

Two generations of anemometers have been fabricated at the Caltech Micromachining Lab. The 1st generation has silicon nitride encapsulating the polysilicon probe wires. The poly wires of the 2nd generation are directly exposed to air and consequently the frequency response has improved by an order of magnitude. Fig 4 shows the fabrication process

flow of the 2nd generation.

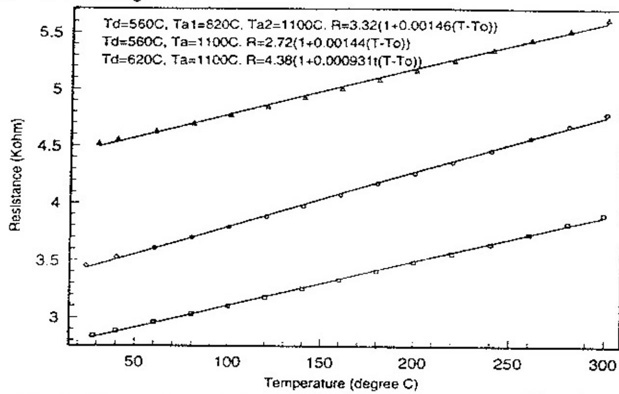

Fig 2. The temperature behavior of boron doped ($2 \times 10^{20} cm^{-3}$) polysilicon resistors (50 squares) under different deposition and annealing conditions.

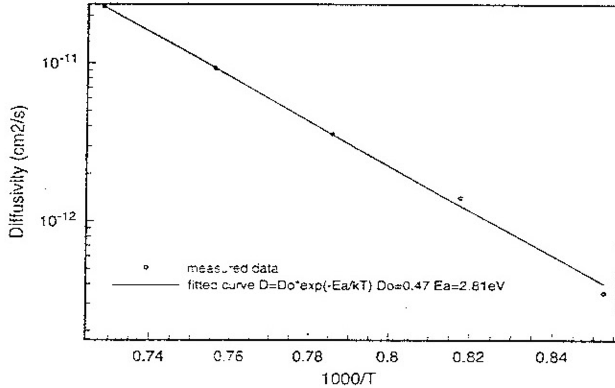

Fig 3. Lateral boron diffusivity at different temperatures in polysilicon deposited at 560°C and annealed at 1100°C.

Two generations of anemometers have been fabricated at the Caltech Micromachining Lab. The 1st generation has silicon nitride encapsulating the polysilicon probe wires. The poly wires of the 2nd generation are directly exposed to air and consequently the frequency response has improved by an order of magnitude. Fig 4 shows the fabrication process flow of the 2nd generation.

The fabrication starts with the oxidation of the (100) Si wafers which have a 10 µm lightly doped epi layer on top of a 8 µm heavily boron doped etch stop layer. A 600 nm thick amorphous Si layer is deposited at 560°C and patterned by plasma etching. Photoresist implantation barriers are then formed on type II poly wires and this is followed by boron ion implantation with a dose of $10^{16} cm^{-2}$ and an energy of 80 keV. After stripping the PR barrier, low dose boron ions ($10^{14} cm^{-2}$) are implanted to dope the center parts of type II wires. Annealing is done at 1100°C for type I wafers and at 900°C for type II wafers for 30 min.. After the aluminum metallization, a 3 µm LTO is deposited at 450°C and the frontside and backside Si substrate windows are opened using both wet and dry etchings. A 10 hours EDP etching at 95°C removes the Si underneath the poly probe. Finally, HNA Si isotropic etchant and pad oxide etchant are used to strip the heavily doped boron layer and the LTO respectively. Fig 5 shows SEM pictures of some hot-wire anemometers fabricated using this process.

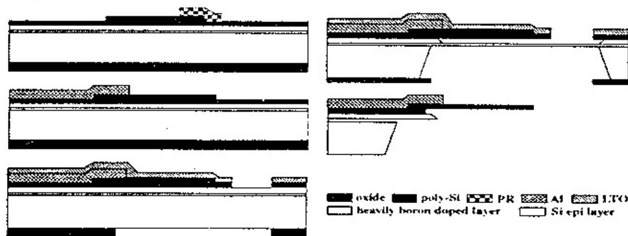

Fig 4. Process flow of polysilicon hot-wire anemometers using both surface and bulk micromachining technologies.

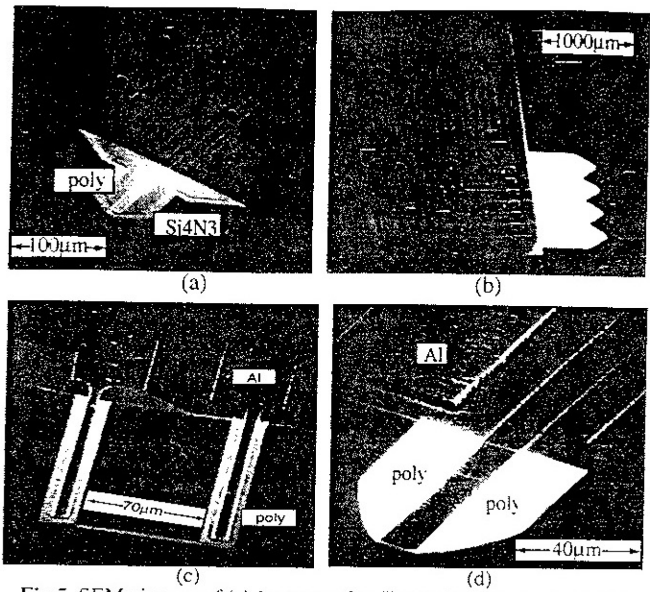

Fig 5. SEM pictures of (a) 1st generation "hot-point anemometer", (b) 1st generation anemometer array for simultaneous velocity distribution measurement, (c) 2nd generation heavily doped anemometer, (d) 2nd generation centerly lightly doped anemometer.

4. THEORY AND EXPERIMENTAL RESULTS

Anemometers can operate either in constant current mode (without feedback) or in constant temperature mode (with feedback). Here, we only use the constant current mode in the early testing stages of our anemometers because of its simplicity. Currently, wind tunnel tests of anemometers in constant temperature mode are under way and will be reported later.

4.1 Time constant

4.1.1 Transient analysis

For a wire with length l, width w and thickness d at some time t and position x from one end, the sum of the heat absorbed by a unit length wire and the heat flowing into it through thermal conduction and convection in unit time must be equal to the ohmic power[10], i.e.,

$$wdc_p \frac{\partial T}{\partial t} - \kappa_{poly} wd \frac{\partial^2 T}{\partial^2 x} + 2h(w+d)(T - T_a) \qquad (1)$$

$$= J^2 \rho_0 wd [1 + \alpha (T - T_a)]$$

where $\rho = 2.32 g/cm^3$, $c_p = 0.7 J/g.°C$, ρ_0, κ_{poly}, $\alpha = 0.0015/°C$ are the density, specific heat, resistivity, thermal conductivity, temperature coefficient of the resistance for the polysilicon, J is the current density, T_a is the ambient temperature. The above differential equation can be solved with the boundary condition $T(0,t) = T(l,t) = T_a$ and initial condition $T(x,0) = T_a$, assuming that the two supports are perfect heat sinks. The solution is a multi-mode response.The first mode determines the time constant,

$$\tau = \tau_1 \tau_2 / (\tau_2 + \tau_2) \qquad (2)$$

$$\tau_1 = \frac{\rho c_p}{\left(-\alpha J^2 \rho_0 + \frac{\kappa_{air} Nu}{wd} \right)}, \tau_2 = \left(\frac{l}{\pi} \right)^2 \frac{\rho c_p}{\kappa_{poly}}$$

where $\kappa_{air} = 2.5 \times 10^{-4} W/cm.°C$ is the thermal conductivity of the air at room temperature. Nu is the *Nusselt* number of the wire. It can be seen from the above expressions that the time constant is due to two components: convection time constant τ_1, which dominates for long wires, and conduction time constant τ_2, which dominates for short wires.

For the centerly lightly doped probes, $\tau \approx \tau_2$ with l being replaced by the effective length of the wire l_{eff}, which is longer than the length of the lightly doped part. However, it is still expected that type II anemometers have a much smaller time constant than type I anemometers since $l_{eff} < L$, which is the total wire length.

4.1.2 Time constant measurement

The time constant is determined by passing a step current through the anemometer in still air and observing the voltage rise (for positive TCR) or fall (for negative TCR) in an oscilloscope. If a steady flow with certain velocity is applied, the time constant will be reduced. For a conventional hot-wire anemometer 5 µm in diameter, the time constant is about 0.5 ms.

Fig 7 shows the time constant in constant current mode of our anemometers for varying wire lengths. The solid line is the fitted curve of Eq. (2) for type I probes. $Nu = 0.78$ and $\kappa_{poly} = 0.26W/cm/^{o}C$ ($0.34W/cm.^{o}C$ in [11]) are the fitting parameters. The fluctuations in the fitted curve are due to the scattering of w from fabrication. The effective width w is calculated from the measured wire resistances with the known sheet resistance of $30\Omega/\square$. There is no curve fit for type II probes, but the measured τ does not change that much for probes with different lengths. From the data we estimated l_{eff} and they range from 15 μm to 38 μm. This large l_{eff} is the result of the low resistivity of the lightly doped part, which was not controlled well in this batch. Note that the 30 μm long probe of this type with a heating τ of only 2 μs and a cooling τ of 8 μs in constant current mode (Fig 7) is currently the fastest anemometer probe.

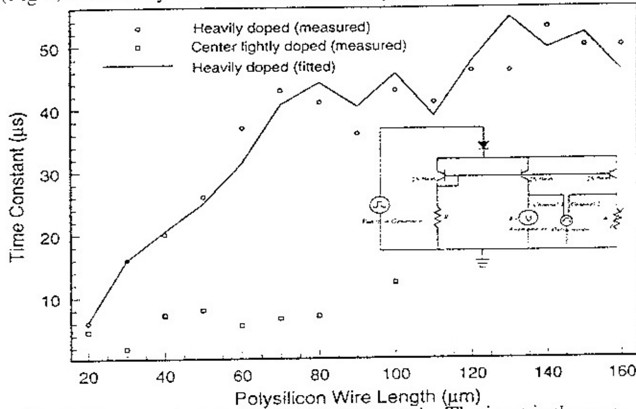

Fig 6. Time constant in constant current mode. The inset is the measurement setup, in which R_c is used to cancel the inherent time delay of the input signal and the circuit.

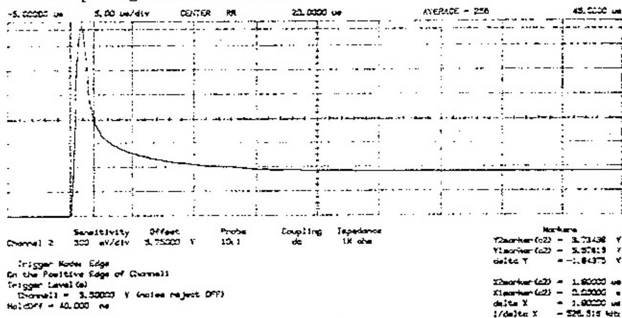

(a) Heating response: $I = 0.4mA, \Delta V \approx 3V, \tau_h = 1.9\mu s$

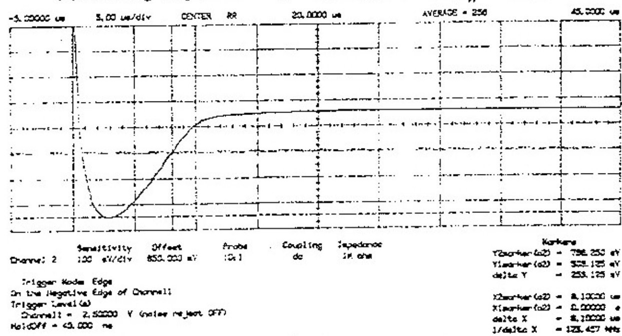

(b) Cooling response: $I = 50\mu A, \Delta V \approx 0.2V, \tau_c = 8.1\mu s$

Fig 7. The time constant is determined by observing the rise or fall of the voltage waveform in oscilloscope when a step current is applied.

4.2 Steady state response

4.2.1 King's law

In steady state, power generation and heat dissipation is balanced, i.e.,

$$IV = K_{eff}(U)(T - T_a) \quad (3)$$

where T is the wire temperature, T_a is the ambient temperature, U is the flow velocity, and $K_{eff}(U)$ is the effective heat transfer coefficient. In a laminar flow, King's law applies,

$$K_{eff}(U) = K_0 + K_1 U^n \quad (4)$$

where K_0 is the heat transfer coefficient which takes into account of conduction, radiation and free convection and is not a function of U. $K_1 U^n$ represents forced convection by the flow boundary layer. The power n depends on the structure and is around 0.5 for conventional hot-wire anemometers. In constant temperature mode, it can be derived from (3) and (4) that

$$V^2 = A_1 + B_1 U^n \quad (5)$$

In constant current mode,

$$T - T_a = \frac{(R - R_a)}{\alpha R_a} = \frac{(V - IR_a)}{\alpha I R_a} = \frac{a}{\alpha}$$

where R_a and α are the resistance and TCR at the ambient temperature, a is the over heat ratio. It can be shown that

$$V = \frac{(A_2 + B_2 U^n)}{(1 + BU^n)} \quad (6)$$

where

$$A_2 = \frac{K_0 I R_a}{(K_0 - \alpha I^2 R_a)},\ B_2 = \frac{K_1}{K_0} A_2,\ B = \frac{K_1}{(K_0 - \alpha I^2 R_a)}$$

Or

$$V_o - V = \frac{AU^n}{(1 + BU^n)} \quad (7)$$

where V_0 is the voltage at $U = 0$, and $A = \frac{K_1 \alpha I^3 R_a^2}{(K_0 - \alpha I^2 R_a)^2}$. If B is small, then

$$V \approx A_2 + B_2 U^n \quad (8)$$

4.2.2 Wind tunnel test

Fig. 8 shows the response of a 70 μm long, heavily doped anemometer (SEM picture in Fig 5(c)) and of a conventional hot-wire anemometer in a wind tunnel at different over heat ratios without any electronic gain. The lines in Fig 8 are the fitted curves of Eq. (7). The sensitivity of our anemometer biased by 2-3 mW is higher than that of the conventional anemometer operating at 4-8 mW. This is due to the smaller size and the higher resistivity of polysilicon over platinum and tungsten. The power n of the velocity U for our anemometer and for the conventional anemometer are around 1.1 and 0.6 respectively. Thus, in comparison with the conventional anemometer, our anemometer has a more linear response and less degradation in sensitivity in the high velocity regime than the conventional anemometer. We believe that this is the result of conduction to the supports which in turn causes nonuniform temperature distribution, a situation which is usually avoided in conventional hot-wire anemometers with large l/d. The directional dependence of the sensitivity has also been tested and the results are shown in Fig 9. The three sets of measured data points at three different angles almost completely overlap. Thus, it is nearly isotropic as long as the angle is not close to 90 degree. This is rather surprising because the theory[1] predicts that the directional dependence of sensitivity follows the cosine law, which is the case of conventional hot-wire anemometers. One possible reason for this might be that the supports have interfered with the flow in our devices.

Fig 10 shows the responses of a 20 μm long type II anemometer at two different angles. It is almost isotropic, but not as much as the heavily doped probe. The near isotropic characteristic can be explained by its short length. Note that it has higher sensitivities than type I even at lower power. Since the I-V curve of type II anemometer is highly nonlinear, it is difficult to estimate the over heat ratio without doing more complicated calibration.

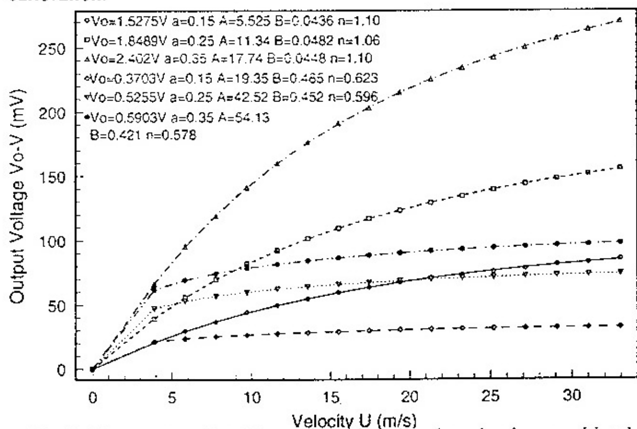

Fig 8. Responses of a 70 μm long heavily doped micromachined (data points represented by circles, squares and triangles) and a conventional (data points represented by diamonds, upside-down triangles and bold dots) hot-wire anemometer in a wind tunnel operating at three different over heat ratios in constant current mode (I = 1.05, 1.22, 1.29 mA for the micromachined, and 10, 13, 14 mA for the conventional, respectively).

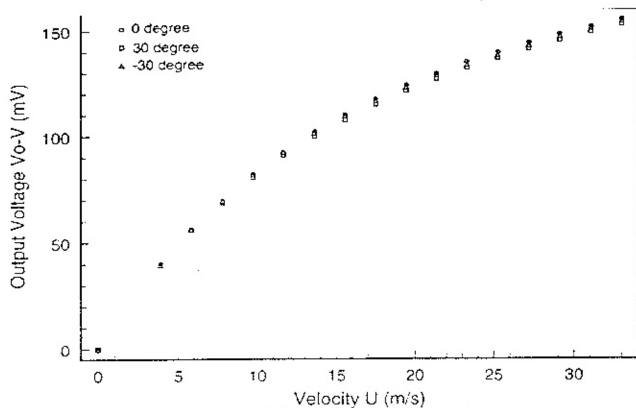

Fig 9. Directional testing of the same 70 μm heavily doped anemometer in constant current mode at I = 1.22 mA with over heat ratio of 0.25. The angle is between the flow and the normal to the wire in the anemometer plane.

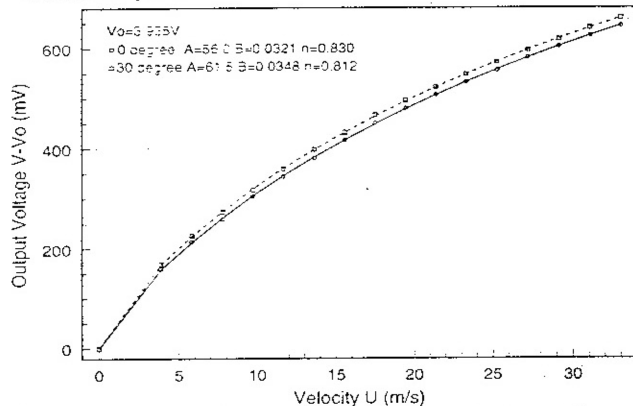

Fig 10. Response of a 20 μm long type II anemometer at two different angles. The average sensitivity is 20 mV/m.s at I = 0.5 mA.

5. DISCUSSION

As previously mentioned in the design section, we found that the stress distribution along the depth of the polysilicon deposited at 620°C and annealed at 1100°C is not uniform. Sometimes, the tips of all the anemometer probes in a wafer made from this type of poly bend up about 50 μm, as shown in Fig 11. However, this phenomenon is never observed in anemometers made from the polysilicon deposited at 560°C and annealed at 1100°C. The reason might be that the structure of as-deposited and as-implanted amorphous silicon films are uniform along the depth. During annealing, the grain growth is uniform, so the stress distribution is uniform too.

Fig 12 shows the temporal drift of a 70 μm long heavily doped probe. The resistance increases slowly. Several factors contribute to the drift. First, the polysilicon is not protected and could be oxidized during high temperature operation. This can be avoided by a conformal anti-oxidation

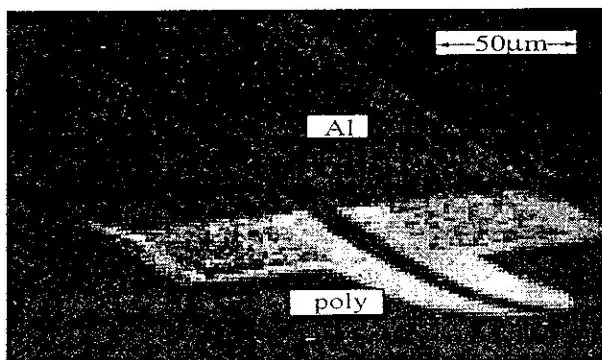

Fig 11. SEM picture of the intrinsically bent anemometer probe

layer coating over the free standing polysilicon structures which only increases the time constant a little. Second, since polysilicon has high diffusivity, the temperature nonuniformity and the electric field across the wire at the operating temperature of a few hundred degrees may cause the slow diffusion of dopants. Amemiya *et al*[12] found that the resistivity of heavily doped polysilicon decreases under high current density. This contradicts our observation. Further study need to be done on the mechanism of this drift.

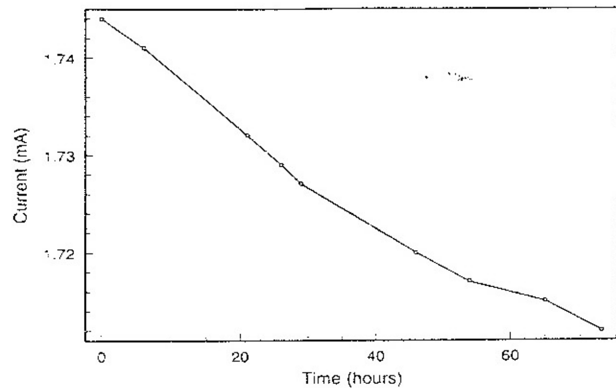

Fig 12. The temporal drift of a 70 μm long heavily doped anemometer at V = 2.5V and a = 0.35.

6. CONCLUSION

Two types of micromachined polysilicon anemometers have been developed. Both have demonstrated superior performance over conventional hot-wire anemometers. Reliability tests and design iterations still need to be done for practical wind tunnel use.

ACKNOWLEDGMENT

This project is supported by AFOSR under Grant F49620-92-J-0424. The authors would like to thank Jianqiang Liu, Chang Liu, Ren Wu and Trevor Roper for many discussions and help in the designing and fabrication.

REFERENCES

[1] R. F. Blackwelder, *Methods of Experimental Physics: Fluid Dynamics*, Vol. 18, Part A, Academic Press, 1981, pp. 259-314.

[2] A. E. Perry, *Hot-Wire Anemometry*, Clarendon Press, Oxford, 1982.

[3] Y. C. Tai, and R. S. Muller, "Polysilicon Bridge for Anemometer Application", *Digest Tech Papers, Transducers '85*, Philadephia, PA, June 4-7, 1985, pp. 354-357.

[4] H. Rahnamai, and J. N. Zemel, "Pyroelectric Anemometers: Preparation and Velocity Measurements", *Sensors and Actuators*, Vol.2, 1981, pp. 3-16.

[5] M. Stenberg, G. Stemme, G. Kittilslad, and K. Pedersen, "A Silicon Sensor for Measurement of Liquid Flow and Thickness of Fouling Biofilms", *Sensors and Actuators*, Vol.13, 1988, pp. 203-221.

[6] B. W. van Oudheusden, and J. H. Huijsing, "Integrated Silicon Flow Direction Sensor", *Sensors and Actuators*, Vol.16, 1989, pp. 109-119.

[7] R. Kersjes, J. Eichholz, A. Langerbein, Y. Manoli, W. Mokwa, "An Integrated Sensor for Invasive Blood-Velocity Measurement", *Sensors and Actuators*, Vol. 37-38, 1993, pp. 674-678.

[8] Y. C. Tai, and R. S. Muller, "Lightly Doped Polysilicon Bridge as a Flow Meter", *Sensors and Actuators*, Vol. 15, No. 1, 1988, pp. 63-75.

[9] G. Harbeke, L. Krausbauer, E. F. Steigmeier, A. E. Widmer, H. F. Kappert and G. Neugebauer, "Growth and Physical Properties of LPCVD Polycrystalline Silicon Films", *J. Electrochem. Soc.*, Vol.131(3), 1984, pp. 675-682.

[10] C. H. Mastrangelo, *M.S. Thesis*, UC Berkeley, 1987.

[11] Y. C. Tai, C. H. Mastrangelo, and R. S. Muller, "Thermal Conductivity of LPCVD Polycrystalline Silicon", *J. Appl. Physics*, Vol. 63, No. 5, 1988, pp. 1442-1447.

[12] Y. Amemiya, T. Ono, and K. Kato, "Electrical Trimming of Heavily Doped Polycrystalline Silicon Resistors", *IEEE Trans. Electron Devices*, Vol. ED-26, No. 11, 1979, pp. 1738-1742.